THE JOURNAL OF COMPARATIVE NEUROLOGY 276:412-422 (1988)

Retinal Ganglion Cell Topography in Teleosts: A Comparison Between Nissl-Stained Material and Retrograde Labelling From the Optic Nerve

SHAUN P. COLLIN AND JOHN D. PETTIGREW
Vision, Touch and Hearing Research Centre, Department of Physiology and Pharmacology, University of Queensland, St. Lucia, Queensland, Australia 4067; Heron Island Research Station, University of Queensland, Heron Island via Gladstone, Queensland, Australia 4680

ABSTRACT

The retinal topography of cells within the ganglion cell layer of three teleost species is examined in Nissl-stained material in which all neuronal elements containing Nissl substance in the cytoplasm are counted. A topographic comparison is made with retrogradely labelled ganglion cells to differentiate the proportion of nonganglion cells not possessing an axon joining the optic nerve. In the three species studied 92%, 80%, and 66% were found to be the maximum proportion of true ganglion cells in the area centralis, horizontal streak, and periphery, respectively. The proportion of nonganglion cells in the total population of cells counted was 24%. The major contribution to this discrepancy is from peripheral nonspecialized regions of the retina. There is little difference in both topography and peak densities of retinal ganglion cells between the two techniques. The soma areas of both populations are analysed, with the homogeneous nonganglion cell population possessing cells between 5 and 15 μm^2 and the heterogeneous ganglion cell soma between 5 and 68 μm^2, increasing in size with eccentricity.

Key words: ganglion cell layer, area centralis, backfilling, fish

Retinal ganglion cell topography, as revealed in a whole mount of the retina, is an unrivalled source of information about the visual capability of a species when it is combined with visual optics (Hughes, '71, '77, '85; Stone and Fukuda, '74). This approach can successfully predict the visual acuity of mammals (Pettigrew et al., '88) and birds (Reymond, '85).

A potential problem with this approach is whether all cells that are counted in the ganglion cell layer are bona fide retinal ganglion cells with a central projection contributing to the visual capability of the species concerned. Retrograde labelling from the central visual nuclei to a retinal whole mount can of course settle this problem (Wong and Hughes, '87) but this approach has problems of its own. First, for rare or inaccessible species it will not always be a routine matter to carry out the retrograde labelling experiment. Nissl-stained retinal material may be the best that is available. This will be true for archival material, for example. Second, subpopulations of retinal ganglion cells, associated with different targets in the brain, may be differentially associated with various aspects of visual behavior in a way which may take a lifetime of work to define in one species alone. There may be value, then, in an approach which sets an upper limit on the visual capabilities of a particular species by counting all the possible ganglion cells, with the caveat that subsequent revision downward may be necessary. The errors involved in such an approach can be defined by extrapolation from other more readily available species and in any case may be small, when compared to the large errors involved in behavioural determinations of visual abilities of animals, especially when one bears in mind that they vary as the square root of the counted density (Pettigrew et al., '88).

In the present account we have tried to define the errors inherent if such an approach is adopted for the teleost retina, whose diverse patterns of organization provide a rich source of comparative material (Collin and Pettigrew,

Accepted May 4, 1988.

'88a,b). Compared with the conventional Nissl-stained retinal material, the preparation of retrogradely labelled retinal whole mounts will not be a routine procedure which we can expect for the unusual species. For this reason we have made a direct comparison between the results obtained with the two techniques in some teleost retinas which exhibit some of the most interesting specializations. We were particularly interested to answer the following questions: Is the striking and unusual pattern of topography we have revealed in the retinal ganglion cell layer of the Labridae and Pomacentridae with Nissl staining a valid representation of the topography revealed in retrogradely stained material in which all retinal ganglion cells have been positively identified? Some critics, more familiar with the larger retinal ganglion cell sizes of the commonly used mammals, were particularly concerned about this question because of the tiny size of putative retinal ganglion cells we have described in the eyes of diurnal teleosts (Collin and Pettigrew, '88a,b). A second question concerns the impact upon any estimation of visual acuity which would occur when nonganglion cells in the retinal ganglion cell layer are excluded from consideration.

Answers to these questions are provided by the results of the present study, which generally support the cautious use of Nissl-stained material in comparative analysis of teleost retinae, as have the results of other studies for mammalian retinae (Wong and Hughes, '87; Pettigrew et al., '88). The general form and positions of specializations such as central areas and streaks, as well as their peak densities, as revealed by retrograde labelling from the optic nerve, are little affected by counting all putative neurons in the ganglion cell layer. On the other hand, since the proportion of nonprojecting neurons increases toward the peripheral "skirts" of the distribution where the contribution is greater in terms of area, there are significant discrepancies between the two techniques if one uses the crude comparison of the total number of putative ganglion cells in the layer. These conclusions are in general agreement with a previous study in the Balistidae and Scorpaenidae families by Ito and Murakami ('84), where optic nerve sectioning and infusion of horseradish peroxidase were used to differentiate ganglion cells. Between 18 and 22% of the ganglion cells could not be accounted for in counts of optic nerve axons. Therefore, it appears that a proportion of nonganglion cells known in cats (Hughes, '85; Wong and Hughes, '87), rats (Perry, '81; Perry et al., '83), mice (Hinds and Hinds, '78), pigeons (Bingelli and Paule, '69; Hayes and Holden, '80), and chickens (Ehrlich and Morgan, '80) may also exist in the retinae of lower vertebrates.

MATERIALS AND METHODS

Retinal whole-mount technique

Two specimens each of the harlequin tusk fish *Lienardella fasciata* (Labridae, 120 mm), the blue tusk fish *Choerodon albigena* (Labridae, 250 mm), and the staghorn damselfish *Amblyglyphidodon curacao* (Pomacentridae, 100 mm) were captured and maintained in the aquaria of the Heron Island Research Station. Each teleost was anesthetized with tricaine methane sulphonate (MS 222, 1:10,000) after being dark adapted for 3 hours. Transcardial perfusion followed and, over a period of 15 minutes, the blood was replaced with 0.1 M phosphate buffer (200 ml) and 4% paraformaldehyde in phosphate buffer (200 ml). The eyes were then excised and the cornea, lens, and vitreous were carefully removed. Each eye was then immersed in 4% paraformaldehyde in phosphate buffer for a further 15 minutes before being transferred to distilled water at 4°C and left overnight. The osmotic shock of this immersion in distilled water allowed the retinae to be easily extricated from the optic capsule devoid of the pigment epithelium. Peripheral slits in the retina allowed it to be flat mounted on a gelatinized slide and dried. Each retinal whole mount was then stained for 8–12 minutes in cold 0.5% cresyl violet, dehydrated, and cleared, and the ganglion cell layer was examined for cells containing Nissl substance. Retinal shrinkage, although not calculated experimentally, is thought be between 1 and 2% with this protocol (Hughes, '75; Mednick and Springer, '88).

Labelling with horseradish peroxidase (HRP)

Two specimens each of *L. fasciata* (120 mm) and *C. albigena* (250 mm) were anesthetized with MS 222 (1:10,000) and placed on a wet platform so that anesthetic and seawater could be continuously passed over the gills via an oxygenation column. The right eye of each fish was rotated nasally and the superior rectus muscle severed to expose the optic nerve. With the aid of a fine stainless-steel hook, the optic nerve was carefully lifted away from the ophthalmic artery and sectioned with a pair of iris scissors. The severed end of the optic nerve was then injected with 50 μl of a solution of 10% HRP in Tris buffer (pH 8.0). The back of the eye was then packed with Gelfoam soaked in HRP solution so that the optic nerve was also bathed in HRP. The eye was then rotated temporally and sutured in its original orientation with 4/0 catgut and, after an application of Sofradex (soframycin and dexamethazone), it was allowed to recover in a constant temperature (26°C) aquarium. After 36 hours the fish were dark adapted for 3 hours, anesthetized with MS 222 (1:5,000), and perfused transcardially. The perfusate consisted of heparinized saline (50 ml) followed by 4% paraformaldehyde in phosphate buffer (100 ml) for 30 minutes. At this stage, the eye was excised and the cornea, lens, and vitreous were removed and the remaining eye capsule was placed into 0.05 M Tris buffer at 4°C overnight. The noninjected left retina was also whole mounted and stained for Nissl substance to enable direct comparisons in eyes of comparable size.

The retinae were carefully dissected from the sclera, choroid, and pigment epithelium. Peripheral slits were made to flat mount each retina onto a gelatinized slide. Temporal, nasal, and dorsal marks were also made for orientation and the retinae were air dried.

Cells injected with HRP were visualized by using a modification to the Hanker-Yates enhancement procedure which incorporates preincubation in a heated 1% solution of cobalt chloride in Tris-HCl buffer. The protocol follows that of Stone ('81). The HRP-filled cells appear brown-black but the intensity was dependent on the relative densities of cells being examined. Shorter incubation times were sometimes necessary to visualize cell soma through the dense array of axons within the nerve fibre layer of the labrids. Retinal whole mounts were then dehydrated, cleared, and mounted in DPX.

Labelling with cobalt lysine

Three specimens of the staghorn damselfish *A. curacao* were anesthetized with MS 222 (1:10,000) and the optic nerve was exposed as in the HRP whole-mount technique. After severing the optic nerve, several injections (a total of 50 μl) of a cobalt-lysine solution were made into the optic

nerve. The solution was prepared according to Lazar ('78): 1.76 g $CoCl_2 \cdot 6H_2O$ and 3.59 g L-lysine base (Sigma: L-5501) are dissolved in 12 ml H_2O by stirring for 24 hours. The pH is adjusted to 7.2 with concentrated HCl and distilled water is added to bring the final volume to 20 ml. The eye was then sutured back into its original orientation and covered with a few drops of Sofradex. Recovery was made in a temperature controlled, well-oxygenated holding tank.

For all fish, survival times of up to 2 days were easily attained and, after dark adaptation for 3 hours, each specimen was reanesthetized with MS 222 (1:5,000) and perfused transcardially with 100 ml of 0.25% ammonium sulphide in Millionig's phosphate buffer (pH 7.4). This was followed by 100 ml phosphate buffer and 100 ml 4% paraformaldehyde in phosphate buffer (pH 7.4). After a total fixation time of 40 minutes, the eye, devoid of cornea, lens, and vitreous, was placed into distilled water at 4°C overnight.

The retina was whole mounted after careful removal of the pigment epithelium, dried, and then intensified by using a slightly modified Gallyas ('79) procedure developed by Bazer and Ebbesson ('84). The intensification solution, which is used at room temperature and in the light, is prepared as follows. Stock solution A: 355 ml distilled water, 1.5 g sodium acetate $\cdot 3H_2O$, 30 ml glacial acetic acid, and 0.5 g silver nitrate. These are mixed overnight and filtered, and 15 ml 1% Triton X-100 is added. Stock solution B: 50 ml 5% sodium tungstate (freshly prepared). Stock solution C: 50 ml 0.25% ascorbic acid (freshly prepared).

The retinae were intensified for up to 18 minutes in two freshly prepared mixtures of eight parts A, one part B, and one part C. Each retina was washed in three changes of distilled water and the silver-intensified projections of the ganglion cells were toned with gold chloride (0.5%) for 15 seconds. Toning was also used to reduce background staining. Three further washes of distilled water and 5 minutes in a 1% sodium thiosulphate solution preceded two more washes in distilled water. The retinae were then dehydrated, cleared, and coverslipped in DPX.

Density distribution maps

Densities of cells stained within the ganglion cell layer stained with cresyl violet, HRP and cobalt-lysine were determined for each retina. The outline of each retinal whole mount was traced onto 1-cm^2 grid paper at a magnification of 20; a Jena DK2 microfiche reader was used, and care was taken to keep the edge of the microscope slide parallel to the grid. The vernier scale on a Leitz Dialux 20 compound microscope was then matched to this grid paper by noting the position of obvious landmarks in the whole mounts. A graticule of 100 squares (magnification calibrated for each objective) placed into the eyepiece was used to define areas for counting at an overall magnification of 500 or 1,000. Numbers of cells within each graticule square were counted every 0.05 mm on the retina. In areas of higher density, cell numbers were counted every 0.025 mm on the retina. These numbers were then converted to cells per mm^2. In this way, up to 500 areas per retina were sampled, allowing determination of small fluctuations in density. Isodensity contours were constructed by interpolation between the values of retinal ganglion cell density.

In those retinae stained for Nissl substance, all recognizable neural elements within the ganglion cell layer were counted. We excluded from the count only elongated cells that contained densely stained nuclei with no Nissl substance in the cytoplasm. These were presumed to be astroglia. All other cellular elements clearly located between the optic nerve fibre layer and the inner nuclear layer that had some Nissl substance in their cytoplasm were counted, independent of size. These distribution maps were then compared with counts of HRP- and cobalt-filled ganglion cells known to possess an axon leaving the retina via the optic nerve.

Determination of cell soma areas

Cell soma areas were calculated by using a camera lucida fitted to a Leitz Dialux 20 compound microscope and an IBM graphics tablet. Cellular images were superimposed onto the graphics tablet and calibrated. By using an electronic stylus, cell soma perimeters were outlined, and computer-assisted area calculations were generated for each cell. A sample of 500 cells was made in each designated area of the retina and collated to produce a histogram of soma area vs. frequency. This area calculation program was also used to determine the total number of cells within the ganglion cell layer over the entire retina. This was made by calculating the area bounded by each isodensity contour and multiplying each area by its average cell density.

RESULTS

Ganglion cell vs. nonganglion cell topography in the harlequin tusk fish *L. fasciata*

Nissl-stained retinae of the harlequin tusk fish possess a highly specialized arrangement of three areae of increased cell density (Fig. 1). An area centralis of over 7.4×10^4 cells per mm^2 lies temporodorsal while a second "area," of 6.0×10^4 cells per mm^2, lies along the retinal meridian, nasal of the falciform process. This second area also extends nasally to form a horizontal streak. The peripheral areas of the retina possess a mean density of 0.75×10^4 cells per mm^2. Cells in the areae centrales are tightly packed into two cellular layers within the ganglion cell layer, in contrast to those cells in the periphery, which are restricted to a single layer (Fig. 2).

In order to compare the proportion of cells within the ganglion cell layer that possess an axon exiting the retina via the optic nerve, HRP was applied to the severed end of the optic nerve and the cell density distribution map was determined for the HRP-filled cell population (Fig. 1).

The topography of HRP-filled cells is remarkably similar to that of the Nissl-stained retina. A temporodorsal area centralis of 6.2×10^4 cells per mm^2 lies in an analogous region to that of the Nissl-stained retina and the second area centralis of 5.7×10^4 cells per mm^2 lies along the retinal meridian and is similarly extended nasally into a horizontal streak. Peripheral regions of the retina possess a mean of 0.42×10^4 cells per mm^2.

Somatal area calculations of cells containing Nissl substance and HRP-filled cells reveal a predominance of cells between 5 and 15 μm^2 within the areae centrales of both retinae (Fig. 3). The largest soma area found for either cell population within the area centralis was 50 μm^2, although cells greater than 22 μm^2 were found in very low proportions (less than 0.4%). However, the cells in the periphery were relatively more heterogeneous in size. Here, the predominant size class in cells containing Nissl substance ranged from 5 to 30 μm^2, while HRP-filled cells were found to be between 10 and 40 μm^2. The largest cells in this region were 100 μm^2. Therefore, there is a population of small

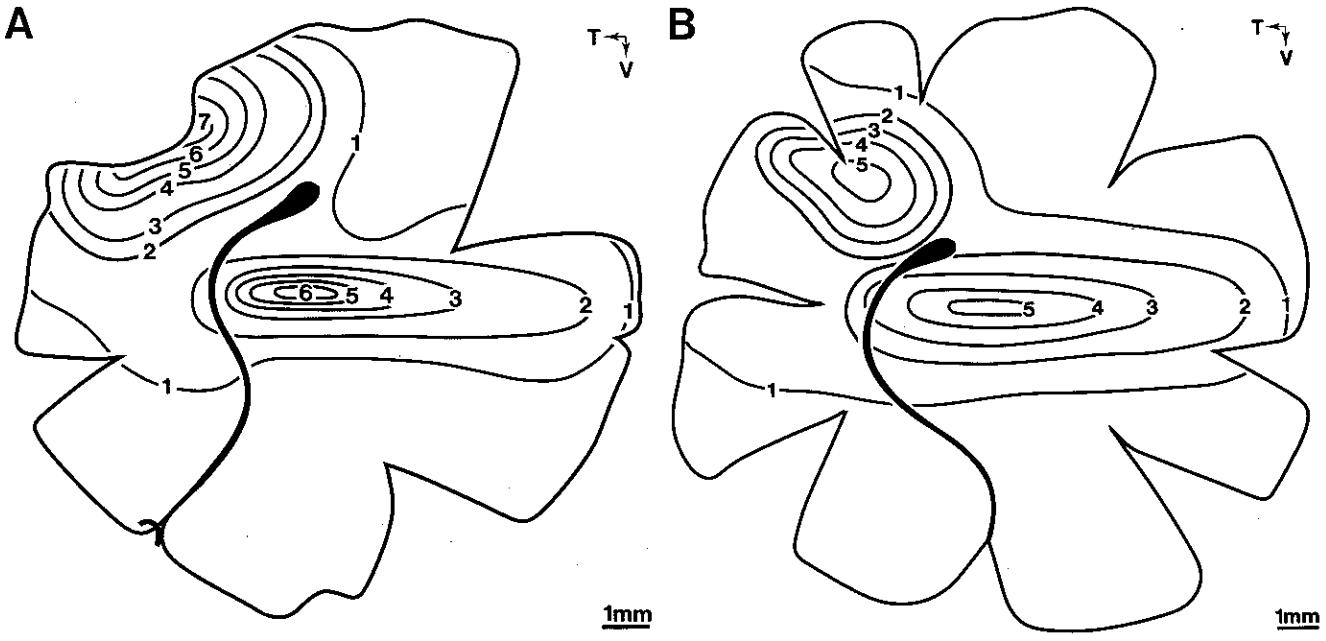

Fig. 1. A: Retinal topography of all cells within the ganglion cell layer containing Nissl substance in the cytoplasm in the right eye of the harlequin tusk fish *Lienardella fasciata*. Note the temporodorsal area centralis of 7.0×10^4 cells per mm^2 with a second area of 6.0×10^4 cells per mm^2 extended along the retinal meridian as a streak. B: Retinal topography of ganglion cells possessing retrogradely labelled HRP from the optic nerve in *L. fasciata*. The topography and peak densities reveal little change between the two techniques. The elongated optic nerve head and curved falciform process are delineated in black. T, temporal; V, ventral.

cells, between 5 and 10 μm^2, in the periphery, that are nonganglion cells (Fig. 3).

Comparisons of cell densities along transects across the retina also reveal relative proportions of nonganglion cells in the area centralis and in the periphery. Transect A-A′ in Figure 4, through the two areae centrales, illustrates the relative densities of cells within the zones of putatively highest visual acuity. The proportion of HRP-filled ganglion cells to those containing Nissl substance is 84% in the temporodorsal area centralis and 92% in the meridianal area centralis. However, the proportion in the nasoventral periphery falls to 40%. Transect B-B′, in comparison, lies across the ventral retina from the temporal perimeter to the nasal perimeter and the relative proportion in this peripheral region is 66%.

Total numbers of cells were calculated for each retina with a computer-assisted program that determines the area bound by each isodensity contour. The total number of cells containing Nissl substance was 1.734×10^6. HRP-filled ganglion cells were calculated to be 1.320×10^6. Therefore,

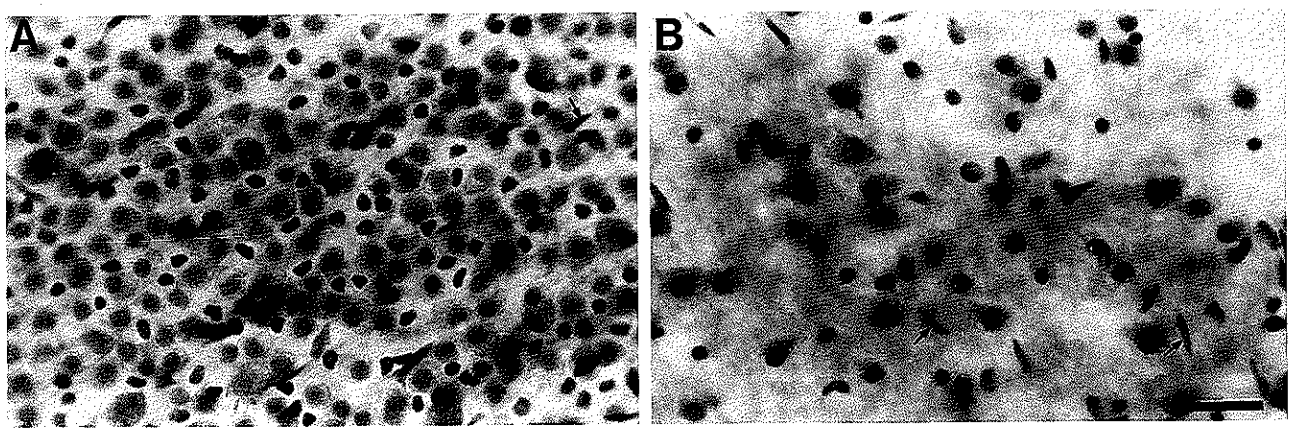

Fig. 2. Light micrographs of Nissl-stained cells within the ganglion cell layer of the blue tusk fish *Choerodon albigena*. Within the horizontal streak (A) cells occur in higher densities with small cell somata in contrast to the heterogeneous soma sizes of cells in the periphery (B). Note the appearance of the presumed astroglia (arrowed), not counted in this study. Scale bar, 20 μm.

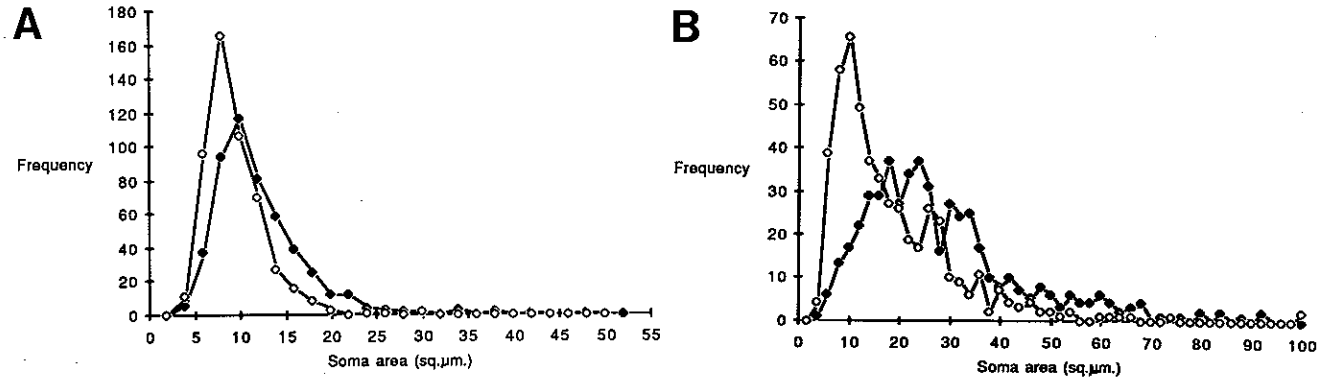

Fig. 3. Plot of soma area vs. frequency of cells within the ganglion cell layer of *L. fasciata* in the region of the temporodorsal area centralis (A) and the ventral periphery (B). The predominant soma size within the area centralis, between 5 and 15 μm^2, is consistent in the Nissl-stained (open diamonds) and HRP-labelled (closed diamonds) populations of cells. However, the periphery possesses a more heterogeneous distribution of soma size with a large population of Nissl-stained cells (nonganglion cells) of between 5 and 40 μm^2. N = 500 cells.

the relative proportion of nonganglion cells within the retina of the harlequin tusk fish *L. fasciata* is 24%.

Ganglion cell vs. nonganglion cell topography in the blue tusk fish *C. albigena*

Studies on *L. fasciata* reveal the differences in true ganglion cell densities throughout the retina. In order to present interspecific variations within different topographic regions of the retina, analysis of the nonganglion cell population within the horizontal streak of *C. albigena* was undertaken.

The retinal topography of the blue tusk fish *C. albigena* (Labridae) has previously been described in Collin and Pettigrew ('88b) (Fig. 5). The retina possesses a similar topography to the closely related *L. fasciata* (Labridae). A temporodorsal area centralis lies at the level of the optic nerve and contains 8.3×10^4 cells per mm^2. A second temporal area centralis of 8.0×10^4 cells per mm^2 is situated near the falciform process and extends along the retinal meridian to form a horizontal streak of between 4.0 and 5.0×10^4 cells per mm^2.

The retinal region outlined by a rectangle in Figure 5 was analyzed in a Nissl-stained retina and retrogradely labelled ganglion cells were stained with HRP via the optic nerve. Cell soma, in all retinae, were tightly packed and lay in two layers within the ganglion cell layer (Fig. 6). The proportion of HRP-filled cells to cells containing Nissl substance at the peak density of the streak was 68%. The corresponding proportion of total ganglion cells counted within the ganglion cell layer within this restricted area was calculated to be 80%.

Soma areas of ganglion cell and nonganglion cell populations were determined and plotted against frequency (Fig. 7). The population of Nissl-stained cells possesses a unimodal size distribution with cells of between 10 and 24 μm^2

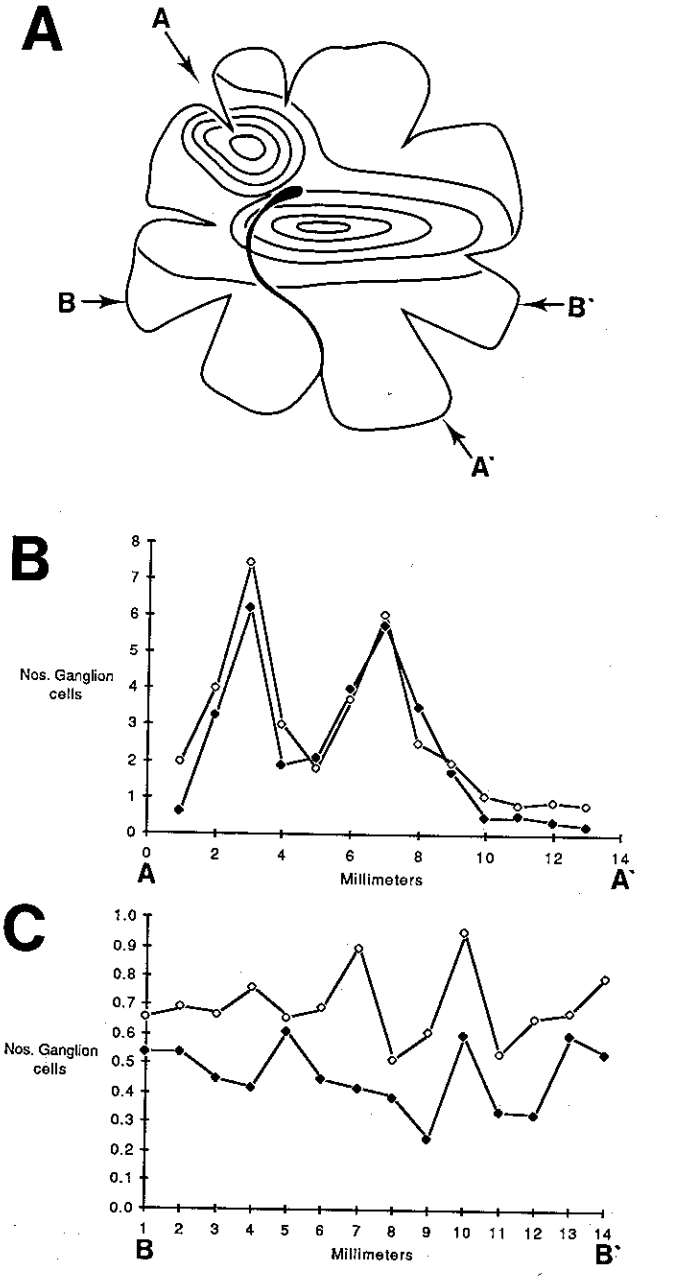

Fig. 4. A: Schematic representation of the retinal topography of the right eye of *L. fasciata* illustrating the transects (A-A′ and B-B′) of analysis of cell frequency vs. eccentricity. B,C: Analysis of transect A-A′ and B-B′ showing the frequency of cells stained either with Nissl (open diamonds) or HRP (closed diamonds) plotted against distance examined in analogous regions of two retinae. Note the close matching of ganglion cell densities in the two areae centrales (B) compared to the relatively large discrepancies in the periphery (C).

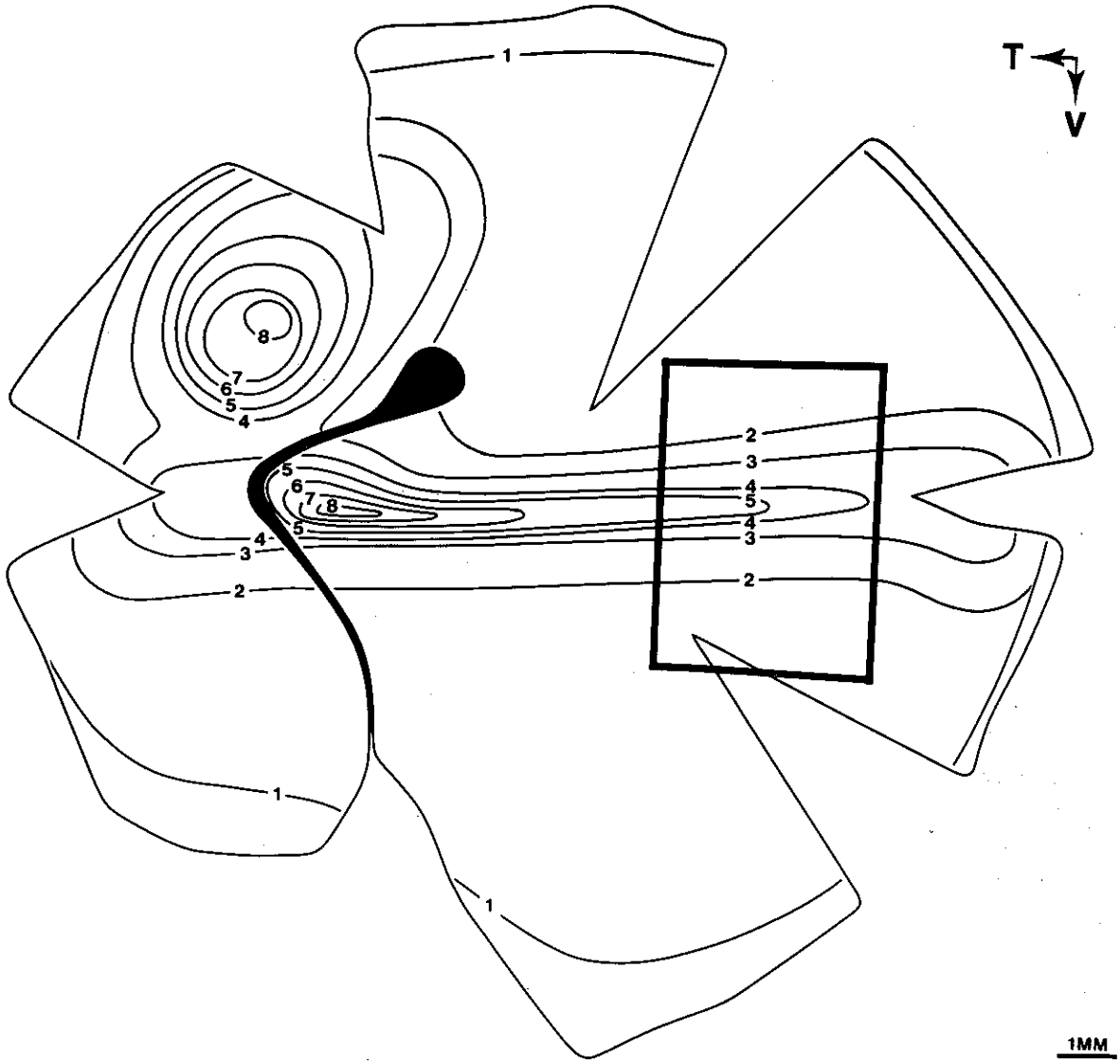

Fig. 5. Retinal topography of Nissl-stained neurons in the right eye of the blue tusk fish *C. albigena*, previously examined by Collin and Pettigrew ('88b). The outlined area of the horizontal streak is reanalyzed in this study to determine the proportion of nonganglion cells by comparing counts of Nissl-stained neurons and HRP-labelled ganglion cells from the optic nerve. Note the intrafamilial similarity between this and the retina of *L. fasciata*. Densities $\times 10^4$ cells per mm^2. T, temporal; V, ventral.

predominating. HRP-filled cells also have a unimodal distribution with the 14- to 38-μm^2 size classes predominating. Therefore, a population of smaller nonganglion cells exists within the ganglion cell layer of *C. albigena*.

Ganglion cell vs. nonganglion cell topography in the staghorn damselfish *A. curacao*

Figure 8 illustrates the retinal topography of cells containing Nissl substance within the ganglion cell layer of the staghorn damselfish *A. curacao* (Collin and Pettigrew, '88a). This retina is less specialized than the previous two examples; it has a centroperipheral gradient of 2 compared to 10 in *C. albigena*. However, three zones of increased cell density are found in the temporal, ventral, and nasodorsal regions of the retina in *A. curacao*. The highest cell density occurs in the ventral area centralis, with over 2.75 $\times 10^4$ cells per mm^2. The remaining retina possesses peripheral densities of between 1.50 and 1.75 $\times 10^4$ cells per mm^2.

The retinal topography of *A. curacao*, previously examined by Collin and Pettigrew ('88a), was reanalyzed within the region bordered by a rectangle in Figure 8. Cobaltous-lysine was injected into the optic nerve and an extended survival period enabled examination of retinal ganglion cell distribution and morphology. The proportion of cobalt-filled ganglion cells in peripheral retina was compared to previously examined Nissl-stained material and found to be 76%.

This improved retrograde labelling technique revealed a heterogeneous population of cells with dendritic arborizations that allowed morphological cell classification (Fig. 9). Each cell was only counted if it possessed an axon leaving the retina via the optic nerve. Soma areas of cobalt-filled

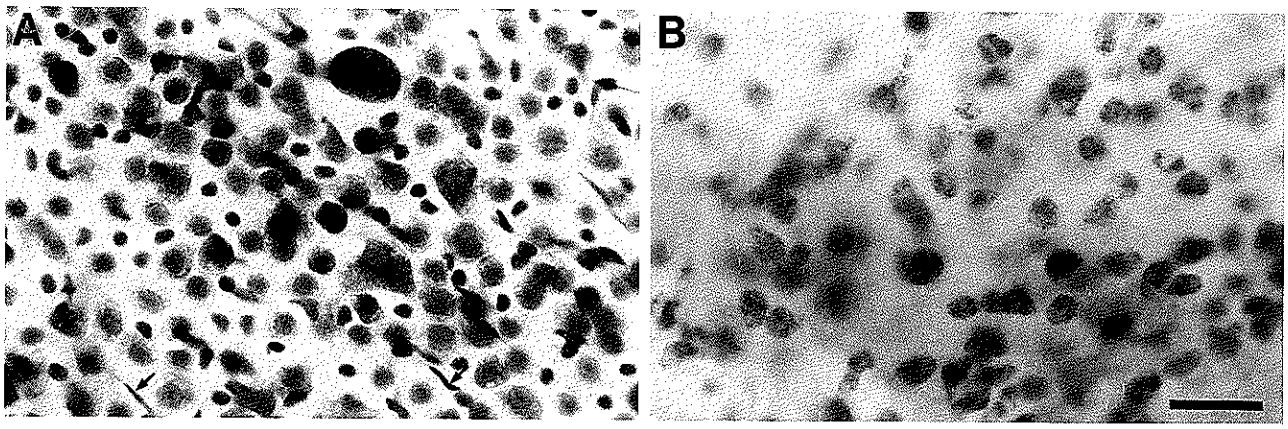

Fig. 6. Light micrographs of neurons within the ganglion cell layer immediately below the peripheral streak region of the blue tusk fish *C. albigena* within the outlined region in Figure 5. Nissl-stained (A) and HRP-labelled (B) cells are presented. The proportion of nonganglion cells in this region was found to be 20% with a population of small-diameter cells and a low number of presumed astroglia (arrowed) evident in the Nissl-stained retina (A). Scale bar, 20 μm.

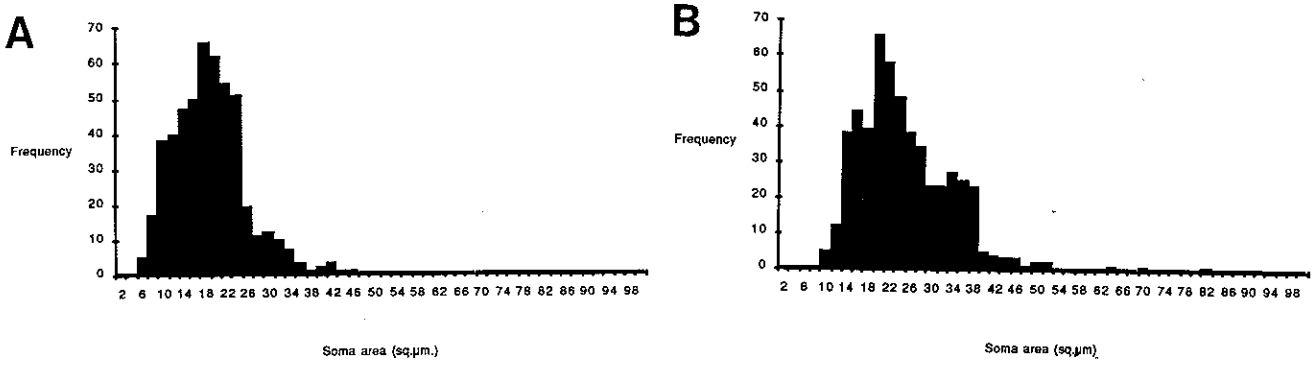

Fig. 7. Histograms of soma area vs. frequency of Nissl-stained (A) and HRP-labelled (B) cells within the peripheral streak of the ganglion cell layer of *C. albigena*. Both populations of cells possess a unimodal distribution with a similar predominant soma size of between 10 and 28 μm^2. However, a population of smaller nonganglion cells and larger HRP-filled ganglion cells can be detected upon close comparison of the two histograms. N = 500 cells.

cells were plotted against frequency (n = 500) and compared to soma areas of Nissl-stained cells (n = 500) over the same area (Fig. 10). Cobalt-filled soma were between 10 and 54 μm^2 in area with a unimodal distribution. Nissl-stained somata had a similar unimodal distribution, although were markedly of smaller area (between 8 and 36 μm^2). Therefore, as in the previous two species, a large nonganglion cell population of smaller soma area exists.

Proportion of ganglion cells to nonganglion cells over the entire retina

The proportion of true ganglion cells to presumed ganglion cells, in the three species studied, is variable in different regions of the retina. However, the topography remains unchanged irrespective of the inclusion of other cell populations in the cell counts. Within the areae centrales, 80–92% of cells counted were found to be true ganglion cells, in *L. fasciata*, while in the periphery a variable proportion of between 40 and 66% was found. The proportion of true ganglion cells over the entire retina of *L. fasciata* and within an area of the nonspecialized retina of *A. curacao* was found to be 76%. If this proportion is adopted for teleosts it could be used to calculate the total populations of ganglion cells within the ganglion cell layer of other species previously examined for Nissl substance. The total ganglion cell population in the ganglion cell layer of *C. albigena* and *A. curacao* (reported in Collin and Pettigrew, '88a,b) would now be 1.511×10^6 and 1.195×10^6, respectively.

Proportions of glial cells

The population of nonganglion cells was not examined to differentiate the proportion of displaced amacrine cells to other association neurons. However, neuroglia were noted to be present in low proportions. Predominantly, astrocyte-like inclusions were found, but distinguishing them from microglia and müllerian glia was difficult on the basis of shape and lack of Nissl substance. The proportion of these

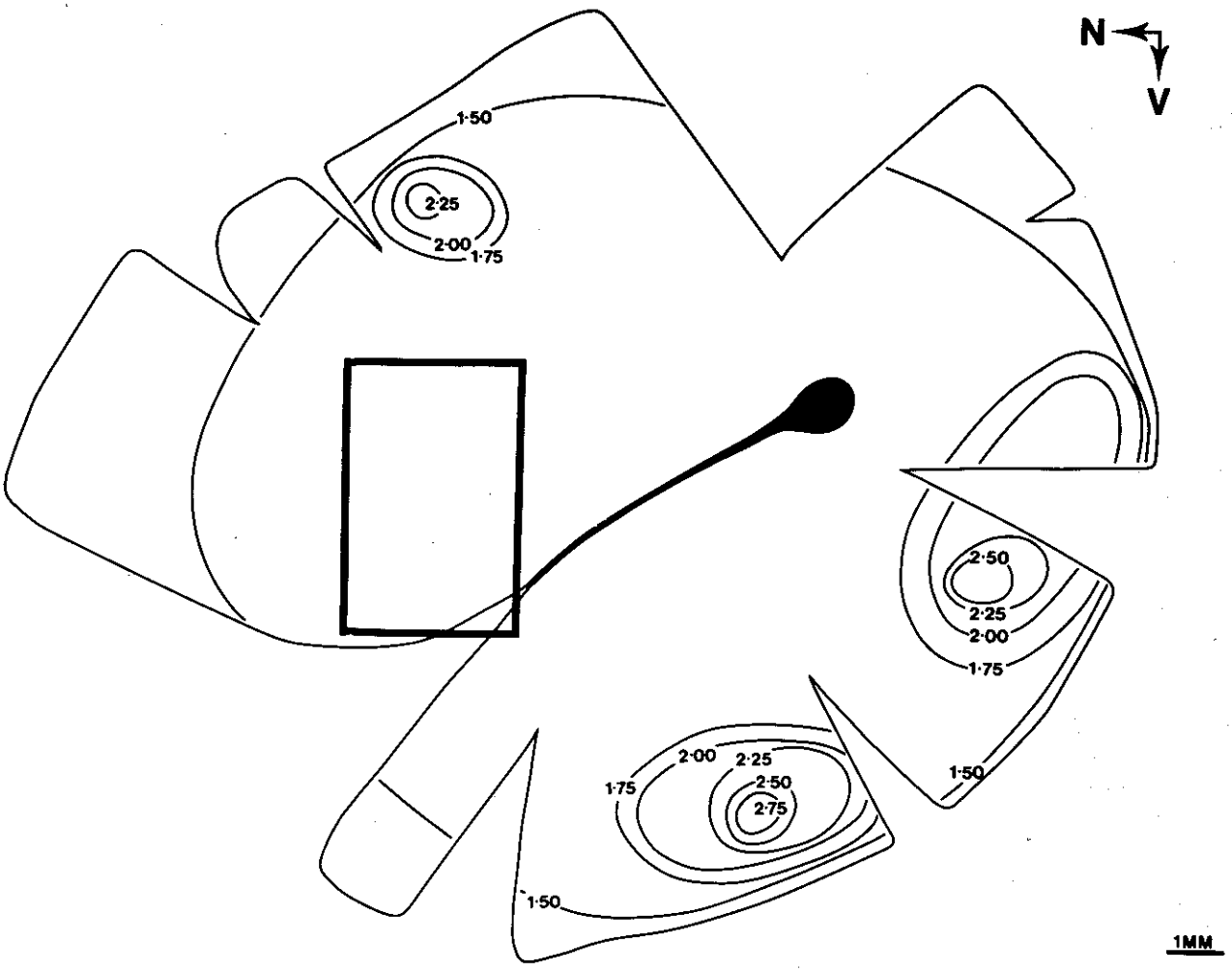

Fig. 8. Retinal topography of Nissl-stained neurons in the left eye of the staghorn damselfish *Amblyglyphidodon curacao*, previously examined by Collin and Pettigrew ('88a). The outlined area of the nonspecialized peripheral region of this retina is reanalyzed in this study to determine the proportion of nonganglion cells by comparing counts of Nissl-stained neurons and cobalt-lysine-labelled ganglion cells from the optic nerve. Note the low cell gradients between the three areae centrales and the periphery. Densities $\times 10^4$ cells per mm^2. N, nasal; V, ventral.

cells was estimated to be only 5% of the total cell population in the ganglion cell layer. These glial cells are not included in any cell counts within this study.

DISCUSSION

Retinal topography in the harlequin tusk fish *L. fasciata* (Labridae)

The previously undescribed retinal topography of *L. fasciata* is consistent with studies in another species of labrid, *C. albigena* (Collin and Pettigrew, '88b). The existence of three retinal specializations is consistent in position, cell density, and total numbers of ganglion cells. Its retinal topography is similar to that of the filefish *Navodon modestus* (Ito and Murakami, '84) although cell densities are much higher in *L. fasciata*. With such a pronounced temporal area centralis some degree of binocular vision would be expected. The extension of a second area into a horizontal streak may be used to maintain a horizontal orientation when feeding in the open environment in which it lives.

Alterations in retinal topography with the inclusion of the nonganglion cell population in cell counts

Comparisons of cell distribution maps of all Nissl-stained cells within the ganglion cell layer to maps of cells labelled with retrogradely labelled HRP reveal the retinal topography in the harlequin tusk fish to be unchanged. The retinal positions of the two areae centrales and the streak across the retinal meridian remain unaltered, with peak densities relatively unchanged in corresponding areae. Therefore, the striking and unusual patterns of topography revealed in the retinal ganglion cell layer of teleosts in Collin and Pettigrew ('88a,b) are valid representations of the visual capabilities of each species since the ganglion cell mosaic provides the only link between the eye and behavioural output (Pettigrew et al., '88).

Limited information exists from other vertebrates on ganglion cell and nonganglion cell topographies in the same species. Classical nonganglion cell neurons described in the cat by Hughes ('75) and in the rabbit by Wieniawa-Narkiewicz ('83) as bar-cells and microneurons have been rede-

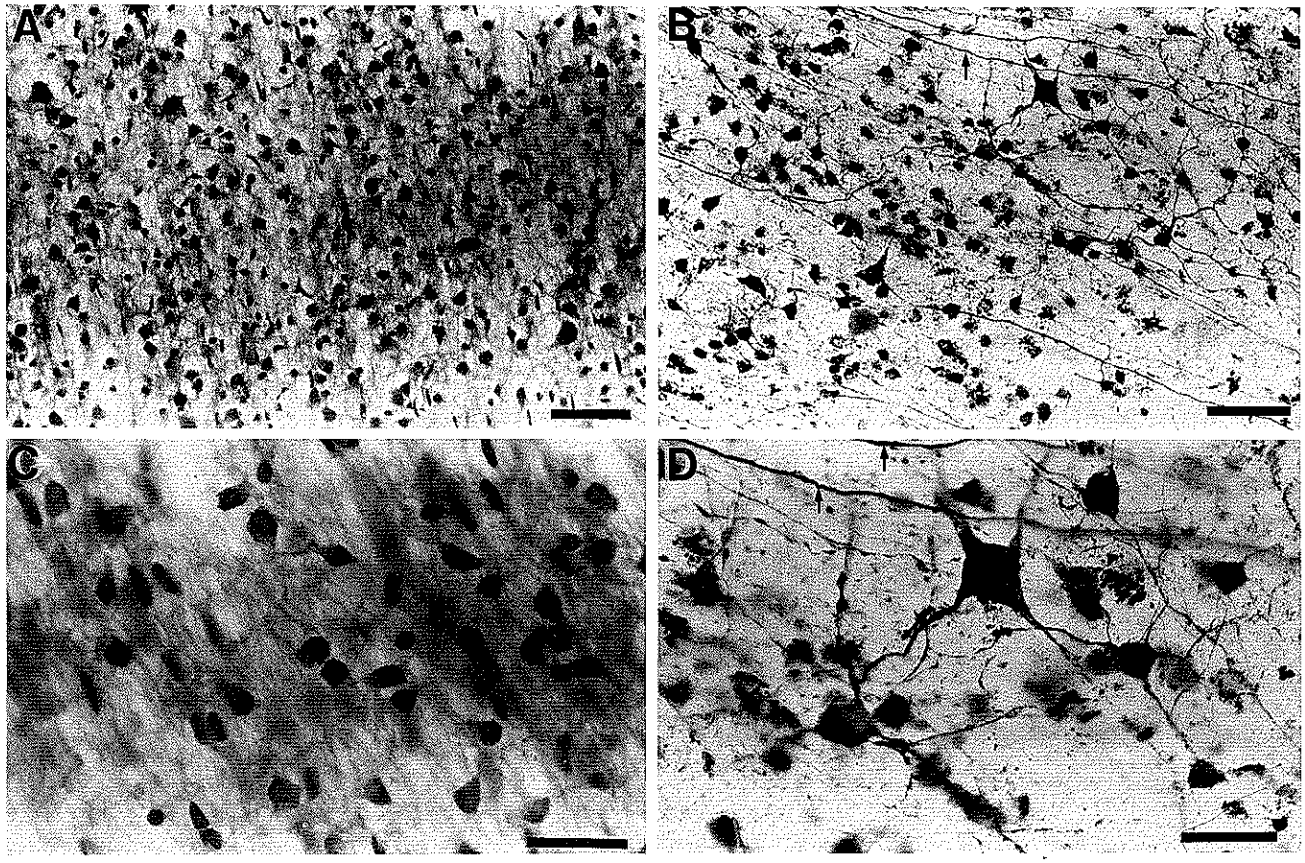

Fig. 9. Light micrographs of Nissl-stained (**A,C**) and cobalt-lysine-labelled (**B,D**) cells in the outlined region of Figure 8. Different ganglion cell classes could be delineated in retrogradely labelled cells which possessed an axon (arrowed) leaving the retina via the optic nerve. Scale bar for A and B is 40 μm; scale bar for C and D is 15 μm.

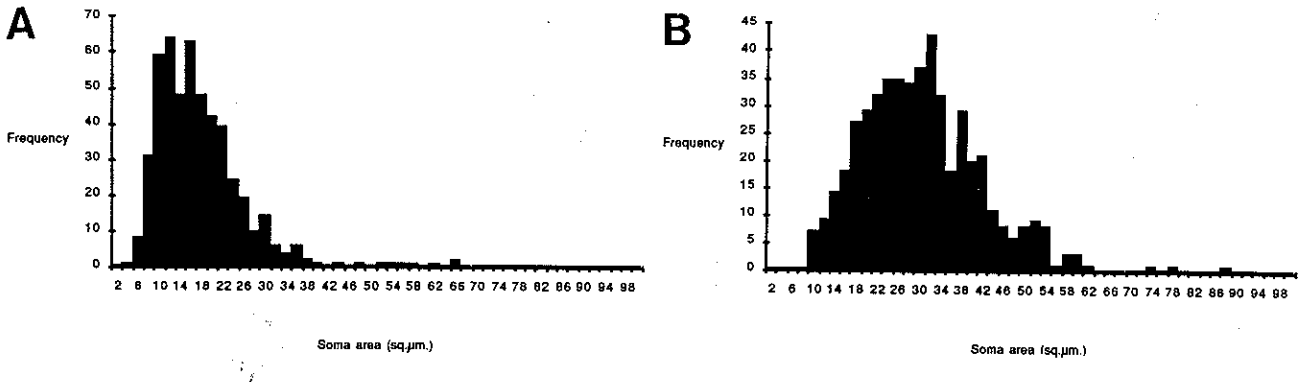

Fig. 10. Histogram plotting soma area vs. frequency of Nissl-stained (**A**) and cobalt-lysine-labelled (**B**) cells in the retina of *A. curacao*. Note each population possesses a unimodal distribution although a large population of smaller nonganglion cells, 8–36μm^2, is revealed in Nissl-stained material. N = 500 cells.

scribed as displaced amacrine cells by Wong and Hughes ('87). Their criteria are that these cells cannot be retrogradely back-filled with HRP, are known to survive optic nerve section, have morphological counterparts within the inner nuclear layer, and based on serial electron microscopic reconstruction, have synapses onto other cells. Wong and Hughes ('87) have examined both populations of cells and find the distribution map of bar-cells and microneurons within the ganglion cell layer to be identical to the distribution maps of true ganglion cells and the total cell population. In this study, detailed analysis of the nonganglion cell population was not undertaken. The relative densities of nonganglion cells increase proportionally with eccentricity from the area centralis. Therefore, the topography of the nonganglion cell population may also be similar to that of the true ganglion cell population but further study is required in order to morphologically differentiate the existence of these other subpopulations.

Proportions of ganglion to nonganglion cell populations

The proportion of ganglion to nonganglion cells decreases with retinal eccentricity. This may vary in specific areas of the retina—for example, near the optic nerve, where older cells have previously been found, in teleosts, to show restricted labelling with HRP (Ito and Murakami, '84). Within the areae centrales of *L. fasciata*, between 84 and 92% of the total cell population within the ganglion cell layer were found to be true ganglion cells. This proportion diminished to 80% within the nasal region of the streak in *L. fasciata* and to 68% within the streak of *C. albigena*. In the periphery, between 40 and 66% of cells possessed an axon exiting the optic nerve. However, over the entire retina, the proportion of ganglion cells within the ganglion cell layer is 76%. Remarkably, this figure was also found to represent the ganglion cell population in the relatively nonspecialized retina of *A. curacao*. Therefore, it is evident that there is little difference between the peak densities, even after the inclusion of the nonganglion cell population, within the areae centralis. The retinal topography is also unchanged. The main differences lie in the peripheral nonspecialized region of the retina which contributes greatly to the discrepancy in total ganglion cell numbers. The importance of quantitatively confirming the proportion of nonganglion cells within the area centralis also establishes the constraints of spatial resolution which can be calculated anatomically in teleosts, using Matthiessen's ratio (Walls, '42).

Recently, in goldfish, the proportion of nonganglion cells was calculated to be 25% in small retinae when cobalt backfilling from the optic nerve (Mednick and Springer, '88) was used. This differentiation of retinal ganglion cells from the total population of hematoxylin-stained cells in the ganglion cell layer was found to diminish in larger retinae. However, the proportion of true ganglion cells increased in the temporal area centralis. Therefore, in the goldfish, as in the three species studied here, the percentage of retinal ganglion cells also changes with eccentricity. The finding that the relative percentages of retinal ganglion cells decrease with retinal size in the goldfish retina (Mednick and Springer, '88) was not investigated in this study, for most specimens were of comparable eye size. However, it is obvious that areas of high cell density within the ganglion cell layer possess higher percentages of ganglion cells for increased visual acuity and that not only temporal retina undergoes some type of differentiation. Whether this differentiation is due to cell death in restricted retinal regions (Sengelaub et al., '86), to a transformation of retinal ganglion cells to displaced amacrine cells (Hinds and Hinds, '83), or to differential retinal growth (Lia et al., '87) is still unknown.

The overall proportion of nonganglion cells in teleosts, in this study (24%), and that of Ito and Murakami ('84) (20%) is similar to other studies on lower vertebrates. The nonganglion cell population in the turtle is very low at 5–6% (Peterson and Ulinski, '79), while more comparable values of 14% are found in both the clawed toad (Graydon and Giorgi, '84) and the burrowing frog (Dunlop and Beazley, '81). In the shovel-nosed ray (Collin, '88) the proportion is higher at 49%, while Nishimura et al. ('79) and Hayes ('84) reveal a maximum of 21% of the total cell population are displaced amacrine cells in birds. A large variation exists in higher vertebrates, with 37–38%, 50–60%, and 81% being nonganglion cells in rabbits (Vaney et al., '81; Hughes, '85), rats (Perry, '81; Perry et al., '83), and cats (Wong and Hughes, '87; Wässle et al., '87), respectively.

Of the proportion of cells not retrogradely labelled, 5% of cells were disregarded in cell counts on the criteria of containing densely stained nuclei with no Nissl substance in their cytoplasm. These cells were thought to be of glial origin, whether they be astrocytes, müllerian glia, or microglia. Most of these astrocytelike cells, as found in the cat (Wong and Hughes, '87) and the rabbit (Schintzer, '85; Hughes, '85), were found within the nerve fibre layer. The remaining cells we presume to be displaced amacrines (Wong and Hughes, '87; Wässle et al., '87).

Soma size of neurons within the ganglion cell layer

The small soma size of the ganglion cells (2.8 μm in diameter in *L. fasciata* and *C. albigena*) accounts for the relatively high ganglion cell densities within the areae centrales. Ganglion cell somata of the sand lance *Limnichthyes fasciatus* (Creeiidae, Perciformes) range in size between means of 8.8 and 11.8 μm^2 in the area centralis and periphery respectively (Collin and Collin, '88). The smallest diameter of these cells is between 4 and 6 μm^2. This is in contrast to a number of other pelagic teleost species that possess large soma of 50 μm^2 in the area centralis (unpublished results).

As ganglion cell density decreases, soma area increases. The smallest somata, between 5 and 24 μm^2, are found in the areae centrales of *L. fasciata*, while peripheral ganglion cells range in size between 5 and 68 μm^2. This change was also found by Ito and Murakami ('84): shifts of the mean ganglion cell soma area of 18.4 to 38.2 μm^2 *(Sebastiscus marmorarus)* and of 23.8 to 52.6 μm^2 *(Navodon modestus)* were found from the area centralis to the periphery. This shift may be a function of ganglion cell dendritic field size, which has been found to increase with eccentricity (Collin, unpublished results; Boycott and Wässle, '74; Kolb et al., '81; Ito and Murakami, '84). However, this size gradient with relation to eccentricity is not evident in the nonganglion cell population.

The soma size of the nonganglion cell population remains remarkably constant at between 5 and 15 μm^2 (Figs. 3, 7, 10) throughout the retina. These values are low in comparison to those in the burrowing frog (Dunlop and Beazley, '81), where the 14% of the cells in the ganglion cell layer that did not fill with HRP were between 5 and 7 μm in diameter; if one assumes the soma to possess a constant radius this would compare with a soma area of between 20

and 38 μm^2. Further analysis is required on the morphological differentiation of these nonganglion cells and on whether they are, in fact, displaced amacrine cells. This could be confirmed by morphological analysis of synapses, at the level of the electron microscope, and by topographical comparison with amacrine cells in the inner nuclear layer which have previously been found to have a modular relationship with a matching population of cells in the ganglion cell layer (Vaney et al., '81; Wong and Hughes, '87; Collin, '88).

ACKNOWLEDGMENTS

This work was supported by grants to J.D. Pettigrew from the Australian Research Grants Scheme and the National Health and Medical Research Council. We wish to thank Dr. I. Lawn and the staff of the Heron Island Research Station for their cooperation.

LITERATURE CITED

Bazer G.T., and S.O.E. Ebbesson (1984) A simplified cobalt-lysine method for tracing axon trajectories in the central nervous system of vertebrates. Neurosci. Lett. *51*:315–318.

Bingelli, R.L., and W.J. Paule (1969) The pigeon retina: Quantitative aspects of the optic nerve and ganglion cell layer. J. Comp. Neurol. *137*:1–18.

Boycott, B.B., and H. Wässle (1974) The morphological types of ganglion cells of the domestic cat's retina. J. Physiol. (Lond.) *240*:397–419.

Collin, S.P. (1988) The retinal structure of the shovel-nosed ray, *Rhinobatos batillum* (Rhinobatidae). Morphology and quantitative analysis of ganglion, amacrine and bipolar cell populations. Exp. Biol. (in press).

Collin, S.P., and H.B. Collin (1988) Topographical analysis of the retinal ganglion cell layer and optic nerve in the sandlance, *Limnichthyes fasciatus* (Creeiidae, Perciformes). J. Comp. Neurol. (in press).

Collin, S.P., and J.D. Pettigrew (1988a) Retinal topography in reef teleosts I. Some species with well developed areae but poorly developed streaks. Brain Behav. Evol. *31*:269–282.

Collin, S.P., and J.D. Pettigrew (1988b) Retinal topography in reef teleosts II. Some species with prominent horizontal streaks and high density areae. Brain Behav. Evol. *31*:283–295.

Dunlop, S.A., and L.D. Beazley (1981) Changing retinal ganglion cell distribution in the frog *Heleioporus eyrei*. J. Comp. Neurol. *202*:221–236.

Ehrlich, D., and I.G. Morgan (1980) Kainic acid destroys displaced amacrine cells in post-hatch chicken retina. Neurosci. Lett. *17*:43–48.

Gallyas, F. (1979) Light insensitive physical developers. Stain Technol. *54*:173–176.

Graydon, M.L., and P.P. Giorgi (1984) Topography of the retinal ganglion cell layer of *Xenopus*. J. Anat. *139*:145–157.

Hayes, B.P. (1984) Cell populations of the ganglion cell layer: Displaced amacrine and matching amacrine cells in the pigeon retina. Exp. Brain Res. *56*:565–573.

Hayes, B.P., and A.L. Holden (1980) Size classes of ganglion cells in the central yellow field of the pigeon retina. Exp. Brain Res. *39*:269–275.

Hinds, J.W., and P.L. Hinds (1978) Early development of amacrine cells in the mouse retina: An electron microscopic serial section analysis. J. Comp. Neurol. *179*:277–300.

Hinds, J.W., and P.L. Hinds (1983) Development of retinal amacrine cells in the mouse embryo: Evidence for two modes of formation. J. Comp. Neurol. *213*:1–23.

Hughes, A. (1971) Topographical relationships between the anatomy and physiology of the rabbit visual system. Doc. Ophthalmol. *30*:33–159.

Hughes, A. (1975) A qualitative analysis of the cat retinal ganglion cell topography. J. Comp. Neurol. *163*:107–128.

Hughes, A. (1977) The topography of vision in mammals. In F. Crescitelli (ed): Handbook of Sensory Physiology, Vol. 7, No. 5. New York: Springer-Verlag, pp. 613–736.

Hughes, A. (1985) New perspectives in retinal organization. In N. Osborne and G. Chader (eds): Progress in Retinal Research, Vol. 4. Oxford: Pergamon Press, pp. 243–313.

Ito, H., and T. Murakami (1984) Retinal ganglion cells in two teleost species, *Sebastiscus marmoratus* and *Navodon modestus*. J. Comp. Neurol. *229*:80–96.

Kolb, H., R. Nelson, and A. Mariani (1981) Amacrine cells, bipolar cells and ganglion cells of the cat retina: A golgi study. Vision Res. *21*:1081–1114.

Lazer, G. (1978) Application of cobalt-filling technique to show retinal projections in the frog. Neuroscience. *3*:725–736.

Lia, B., R.W. Williams, and L.M. Chalupa (1987) Formation of retinal ganglion cell topography during prenatal development. Science *236*:848–851.

Mednick, A.S., and A.D. Springer (1988) Asymmetric distribution of retinal ganglion cells in goldfish. J. Comp. Neurol. *268*:49–59.

Nishimura, Y., Y. Inoe, and K. Shimai (1979) Morphological development of retinal ganglion cells in the chick embryo. Exp. Neurol. *64*:44–60.

Perry, V.H. (1981) Evidence for an amacrine cell system in the ganglion cell layer of the rat retina. Neuroscience *6*:931–944.

Perry, V.H., Z. Henderson, and R. Linden (1983) Postnatal changes in retinal ganglion cell and optic axon populations in the pigmented rat. J. Comp. Neurol. *219*:356–368.

Peterson, E.H., and P.S. Ulinski (1979) Quantitative studies of the retinal ganglion cells in a turtle, *Pseudemys scripta elegans*. J. Comp. Neurol. *186*:17–42.

Pettigrew, J.D., B. Dreher, C.S. Hopkins, M.J. McCall, and M. Brown (1988) Peak density and distribution of ganglion cells in the retinae of microchiropteran bats: Implications for visual acuity. Brain Behav. Evol. *32* .

Reymond, L. (1985) Spatial visual acuity of the eagle, *Aguila audax*: A behavioural, optical and anatomical investigation. Vision Res. *25*:1477–1491.

Schnitzer, J. (1985) Distribution and immunoreactivity of glia in the retina of the rabbit. J. Comp. Neurol. *240*:128–142.

Sengelaub, D.R., R.P. Dolan, and B.L. Finlay (1986) Cell generation, death, and retinal growth in the development of the hamster retinal ganglion cell layer. J. Comp. Neurol. *246*:527–543.

Stone, J. (1981) The Wholemount Handbook: A Guide to the Preparation and Analysis of Retinal Wholemounts. Sydney: Maitland Publications.

Stone, J., and Y. Fukuda (1974) Properties of cat retinal ganglion cells: A comparison of W-cells with X- and Y-cells. J. Neurophysiol. *37*:722–748.

Vaney, D.I., L. Peichl, and B.B. Boycott (1981) Matching populations of amacrine cells in the inner nuclear and ganglion cell layers of the rabbit retina. J. Comp. Neurol. *199*:373–391.

Walls, G.L. (1942) The Vertebrate Eye and Its Adaptive Radiation. New York: Hafner, 262 pp.

Wässle, H., M.H. Chun, and F. Müller (1987) Amacrine cells in the ganglion cell layer of the cat retina. J. Comp. Neurol. *265*:391–408.

Wieniawa-Narkiewicz, E. (1983) Light and Electron Microscopic Studies of Retinal Organisation. PhD Thesis. A. N. U., Canberra.

Wong, R.O.L., and Hughes, A. (1987) The morphology, number, and distribution of a large population of confirmed displaced amacrine cells in the adult cat retina. J. Comp. Neurol. *255*:159–177.